Competition of magnetic ordering in the U- t-t' model

1998 J. Phys.: Condens. Matter 10 1393

(http://iopscience.iop.org/0953-8984/10/6/022)

J. Phys.: Condens. Matter **10** (1998) 1393–1401. Printed in the UK PII: S0953-8984(98)83492-9

Competition of magnetic ordering in the U–t–t' model

R E Hetzel and P Topalis

Institut für Theoretische Physik, Technische Universität Dresden, D-01062 Dresden, Germany

Received 17 April 1997, in final form 15 October 1997

Abstract. Using the projector quantum Monte Carlo method, we investigate the magnetic properties of the half-filled two-dimensional U–t–t' model on a square lattice. In particular, we describe the transition between the usual antiferromagnetic order and a new, antiferromagnetically layered type of order as a function of the diagonal hopping amplitude t'. In the case of strong correlations U, our results compare favourably to analytical and numerical results on the J_1–J_2 model. Furthermore, we investigate the magnetic ground-state properties for medium correlation strength, too. In this regime, as well as in the strongly correlated case, the system undergoes a transition from antiferromagnetic order to layered antiferromagnetic order at $t'^2 \approx 0.5t^2$.

1. Introduction

The discovery of high-temperature superconductivity [1] has renewed interest in strongly correlated electronic systems. As a simple model for the copper oxide planes, the Hubbard model [2] with nearest-neighbour hopping is often investigated. To reproduce x-ray absorption spectra [3] and magnetic neutron scattering data [4] as well as the Fermi surface of the cuprates, it was proposed to introduce in addition to the nearest-neighbour hopping a diagonal hopping, whose amplitude t' is material dependent. The addition of the diagonal hopping term also has the advantage of distinguishing hole-doped from electron-doped systems, since it destroys the particle–hole symmetry of the original model.

One possible good, numerical method for studying the properties of strongly correlated systems is the quantum Monte Carlo method. Several electronic and magnetic properties of the 2D Hubbard and 2D U–t–t' model on the square lattice have been calculated using the grand canonical quantum Monte Carlo algorithm [5–10]. Some important results of these studies are as follows.

(i) At half-filling the bare Hubbard model has long-range antiferromagnetic order for all values of the on-site repulsion with $U > 0$. If the system is doped, the antiferromagnetic order is destroyed for all $U > 0$ [5, 7–9].

(ii) At half-filling the U–t–t' model develops long-range antiferromagnetic order upon reaching a critical on-site repulsion U_c, which depends on the diagonal hopping t' [6]. If the system is doped, the antiferromagnetic order decreases until incommensurable features appear in the structure factor [6, 10]. Recently, numerical data were reported which suggest the existence of an antiferromagnetic metallic ground state for the U–t–t' model [11].

In the limit of large U and at half-filling, the U–t–t' model maps onto the Heisenberg antiferromagnet with nearest-neighbour and next-nearest-neighbour spin exchange, the so-called J_1–J_2 model. This model, too, has often been investigated in connection with

0953-8984/98/061393+09$19.50

properties of the high-temperature superconducting materials, using a variety of numerical [12–15] and analytical [16] methods. The numerical results were obtained by exact diagonalization of systems of $N = 16$–20 lattice sites [12, 13, 15] up to $N = 6 \times 6$ sites [14]. All of these numerical investigations agree that the system shows a transition from antiferromagnetic to layered antiferromagnetic order, but due to strong finite-size effects it is not clear of what kind the intermediate phase is. Recently, the J_1–J_2 model was investigated [16] in the framework of the cumulant approach [17] giving good agreement with numerical results from exact diagonalization [12, 15].

In this paper, we calculate the staggered and layered magnetizations of the U–t–t' model for several values of the on-site repulsion U using the projector quantum Monte Carlo method [18]. The convergence of this method depends strongly on the initial trial state used. Therefore we have used the spin-density-wave (SDW) ground state [19, 20] as a trial wave function, which, in the case of the bare Hubbard model at half-filling, has the advantage of avoiding the so-called 'minus-sign' problem. In contrast to other SDW mean-field approaches for the U–t–t' model [10], the SDW mean-field solution that we construct here has two variational parameters, namely the staggered and the layered magnetizations m_Q and m_X.

In previous work by Duffy and Moreo [10, 11], the U–t–t' model was investigated in a parameter region of small t' for which the model displays only antiferromagnetic ordering. The case of small t' is believed to be relevant for the high-T_c cuprate superconductors. Furthermore, the antiferromagnetic ordering is why the authors of references [10, 11] restrict their SDW mean-field approximation to the antiferromagnetic solution in the case of half-filling. In contrast, we focus in our work on the transition from antiferromagnetic to layered antiferromagnetic order on varying t' at fixed correlation strength U, thus allowing for unphysically large values of t'. Hence, when constructing a SDW mean-field solution, we include both types of ordering. Our mean-field solution is solely used as a starting point for the quantum Monte Carlo algorithm.

2. The projector quantum Monte Carlo algorithm

Here we briefly review the projector quantum Monte Carlo (PQMC) method for fermions in the ground state. For a detailed discussion, the reader is referred to reference [18].

The key idea of the PQMC algorithm is to project out the ground-state wave function $|\Psi_0\rangle$ of a lattice fermion Hamiltonian H from a given trial wave function $|\Phi_T\rangle$ by applying the operator $\exp(-\beta H)$ to $|\Phi_T\rangle$ according to

$$\lim_{\beta\to\infty} \frac{\mathrm{e}^{-\beta H}|\Phi_T\rangle}{\sqrt{\langle\Phi_T|\mathrm{e}^{-2\beta H}|\Phi_T\rangle}} = |\Psi_0\rangle \frac{\langle\Psi_0|\Phi_T\rangle}{|\langle\Psi_0|\Phi_T\rangle|}. \tag{1}$$

The expectation values of the physical quantities A are then obtained from

$$\langle A\rangle = \lim_{\beta\to\infty} \frac{\langle\Phi_T|\mathrm{e}^{-\beta H} A \mathrm{e}^{-\beta H}|\Phi_T\rangle}{\langle\Phi_T|\mathrm{e}^{-2\beta H}|\Phi_T\rangle}. \tag{2}$$

We consider the two-dimensional Hubbard model on a square lattice where the Hamiltonian H is given by

$$H = \sum_{ij,\sigma} t_{ij} c^{\dagger}_{i\sigma} c_{j\sigma} + \frac{U}{2} \sum_{i,\sigma} n_{i\sigma} n_{i-\sigma} = K + V \tag{3}$$

and t_{ij} denotes nearest-neighbour hopping. In the case of the U–t–t' model the hopping amplitude takes the values

$$t_{ij} = \begin{cases} -t & \text{if } i,\ j \text{ are nearest neighbours} \\ -t' & \text{if } i,\ j \text{ are next-nearest neighbours} \\ 0 & \text{otherwise.} \end{cases}$$

Applying the Trotter–Suzuki decomposition [21, 22] and the discrete Hubbard–Stratonovich transformation [23] to the projection operator, the effect of the projection operator on the trial state can be symbolically rewritten as a sum over the Hubbard–Stratonovich spins $\boldsymbol{S}$:

$$\mathrm{e}^{-\beta H}|\Phi_T\rangle = \sum_{\{\boldsymbol{S}\}} F(\boldsymbol{S})|\Phi_T\rangle.$$

The expectation value of the physical quantity is then obtained from

$$\langle A\rangle = \left(\sum_{\{\boldsymbol{S},\boldsymbol{S}'\}} \langle\Phi_T|F(\boldsymbol{S})AF(\boldsymbol{S}')|\Phi_T\rangle\right) \Big/ \left(\sum_{\{\boldsymbol{S},\boldsymbol{S}'\}} \langle\Phi_T|F(\boldsymbol{S})F(\boldsymbol{S}')|\Phi_T\rangle\right). \tag{4}$$

To evaluate these sums, the Monte Carlo method is used [24], utilizing $|\omega(\boldsymbol{S},\boldsymbol{S}')| = |\langle\Phi_T|F(\boldsymbol{S})F(\boldsymbol{S}')|\Phi_T\rangle|$ as the probability of flipping spins. Since in general $\omega(\boldsymbol{S},\boldsymbol{S}')$ can be negative for some spin configurations $\boldsymbol{S}$, it can be difficult to evaluate equation (4) numerically. This problem is often referred to as the 'minus-sign' problem.

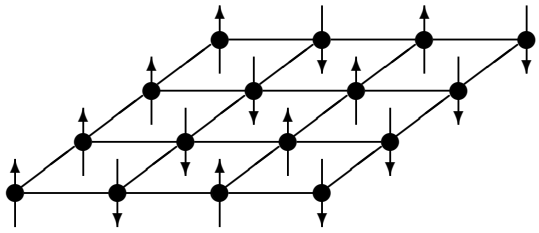

Figure 1. Layered antiferromagnetic order on a square lattice.

3. The spin-density-wave approach for the U–t–t' model

All quantum Monte Carlo simulations suffer from the so-called 'minus-sign' problem though it does not always occur at half-filling. In the PQMC scheme, the 'minus-sign' problem can be avoided for the bare Hubbard model at half-filling if one uses a SDW ground state as the trial wave function. In our simulations, we found that an appropriately chosen SDW ground-state wave function reduces the 'minus-sign' problem in the case of the U–t–t' model, too. In the usual SDW mean-field approach for the U–t–t' model, only the staggered magnetization m_Q of 'normal' antiferromagnetic order is taken into account as a variational parameter [10]. In this work we develop a SDW mean-field approach with two variational parameters, the first being the staggered magnetization m_Q and the second being the layered magnetization m_X. Here m_X is the order parameter for layered antiferromagnetic order. Consider the two sublattices of a chequerboard. If the spins on each sublattice separately are ordered antiferromagnetically, one speaks of *layered antiferromagnetic* order (see figure 1). Spins are then pointing row-wise or column-wise up and down in the z-direction.

We want to present the formal aspects of our SDW approach only briefly. Our starting point is the approximation of the full Hamiltonian (3) in terms of a self-consistent-field Hamiltonian H_{SCF}:

$$H_{SCF} = \sum_{ij,\sigma} t_{ij} c_{i\sigma}^{\dagger} c_{j\sigma} + U \sum_{i,\sigma} \langle n_{i\sigma} \rangle n_{i,-\sigma} + E_0 \tag{5}$$

where $E_0 = -U \sum_i \langle n_{i\uparrow} \rangle \langle n_{i\downarrow} \rangle$ is a constant energy shift. In contrast to the usual *ansatz* for $\langle n_{i\sigma} \rangle$ in the SDW approach, we include not only the staggered magnetization m_Q but also the layered magnetization m_X. Assuming a half-filled square lattice, we write

$$\langle n_{i\sigma} \rangle = \frac{1}{2}(1 + \sigma m_Q \mathrm{e}^{-\mathrm{i}\boldsymbol{Q}\cdot\boldsymbol{R}_i} + \sigma m_X \mathrm{e}^{-\mathrm{i}\boldsymbol{X}\cdot\boldsymbol{R}_i}) \tag{6}$$

where $\boldsymbol{Q} = (\pi, \pi)$ is the antiferromagnetic vector and $\boldsymbol{X} = (\pi, 0)$ is the layered antiferromagnetic vector in $\boldsymbol{k}$-space. Inserting this *ansatz* into H_{SCF}, we obtain in $\boldsymbol{k}$-space

$$H_{SDW} = \sum_{\boldsymbol{k},\sigma}{}'' \boldsymbol{c}_{\boldsymbol{k}\sigma}^{\dagger} \mathbf{H} \boldsymbol{c}_{\boldsymbol{k}\sigma} + E_0 \tag{7}$$

where $\boldsymbol{c}_{\boldsymbol{k}\sigma}^{\dagger} = (c_{\boldsymbol{k}\sigma}^{\dagger}, c_{\boldsymbol{k}+\boldsymbol{Q}\sigma}^{\dagger}, c_{\boldsymbol{k}+\boldsymbol{X}\sigma}^{\dagger}, c_{\boldsymbol{k}+\boldsymbol{Y}\sigma}^{\dagger})$ and

$$\mathbf{H} = \begin{pmatrix} e_1 + e_2 + e_3 + \tilde{U} & \sigma m_Q \tilde{U} & \sigma m_X \tilde{U} & 0 \\ \sigma m_Q \tilde{U} & -e_1 - e_2 + e_3 + \tilde{U} & 0 & \sigma m_X \tilde{U} \\ \sigma m_X \tilde{U} & 0 & -e_1 + e_2 - e_3 + \tilde{U} & \sigma m_Q \tilde{U} \\ 0 & \sigma m_X \tilde{U} & \sigma m_Q \tilde{U} & e_1 - e_2 - e_3 + \tilde{U} \end{pmatrix} \tag{8}$$

with $e_1 = -2t \cos k_x$, $e_2 = -2t \cos k_y$, $e_3 = -4t' \cos k_x \cos k_y$, $\tilde{U} = U/2$ and $\boldsymbol{Y} = (0, \pi)$. Note that the sum in equation (7) runs over the bisected magnetic Brillouin zone, i.e. over one quarter of the full Brillouin zone (see figure 2).

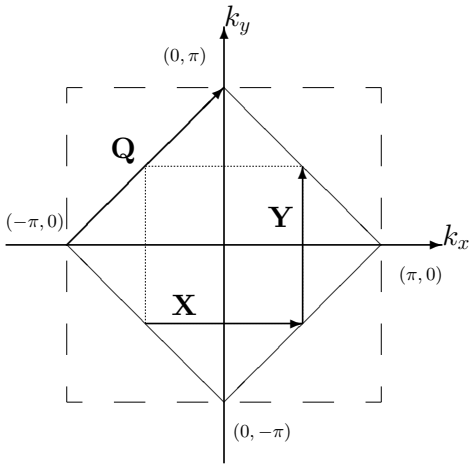

Figure 2. The full Brillouin zone (dashed line), magnetic Brillouin zone (solid line) and Brillouin zone reduced by AF and layered AF order (dotted line) for a square lattice.

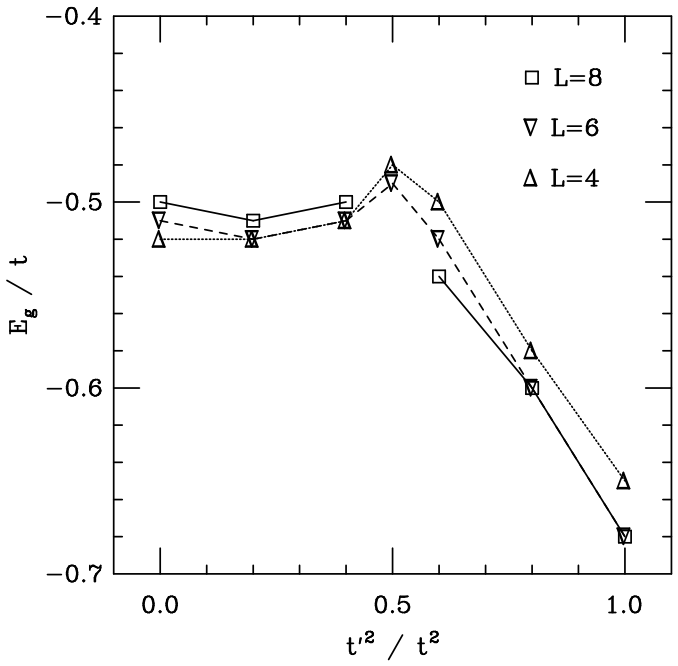

Figure 3. The ground-state energy per site of the U–t–t' model on a square lattice for $U = 8t$. The error bars are of the order of twice the symbol size. Lines are purely guides to the eye.

The parameters m_Q and m_X are determined by iteration from the coupled pair of self-consistent equations

$$m_Q = \frac{1}{N}\sum_i \mathrm{e}^{-\mathrm{i}\boldsymbol{Q}\cdot\boldsymbol{R}_i}\langle n_{i\uparrow} - n_{i\downarrow}\rangle$$
$$m_X = \frac{1}{N}\sum_i \mathrm{e}^{-\mathrm{i}\boldsymbol{X}\cdot\boldsymbol{R}_i}\langle n_{i\uparrow} - n_{i\downarrow}\rangle \tag{9}$$

where $\langle n_{i\uparrow}\rangle$ and $\langle n_{i\downarrow}\rangle$ are themselves functions of m_Q and m_X. The iteration procedure may lead to several fixed points, of which the one of lowest energy is chosen. Finally these values are used for the diagonalization of Hamiltonian (7) to construct the SDW ground state which serves as the trial-state wave function in the projection algorithm.

4. Numerical results

Using the PQMC scheme, we compute the expectation values of H and $n_{i\sigma}$ for the U–t–t' model. On average, we use 64 000 Monte Carlo sweeps per run for one set of parameters. The 'minus-sign' problem, on account of which statistical averages become poor, is in general not serious for values $t' > 0$, except for the region $0.4 \leqslant t'^2/t^2 \leqslant 0.8$. To ensure proper convergence of the algorithm, we have computed the expectation values for different values of β. Typically, the expectation values become independent of β at around $\beta = (5 \ldots 10)t^{-1}$. The number of Trotter slices is chosen to be 512, large enough that the error in our results due to the Trotter decomposition is smaller than the statistical error.

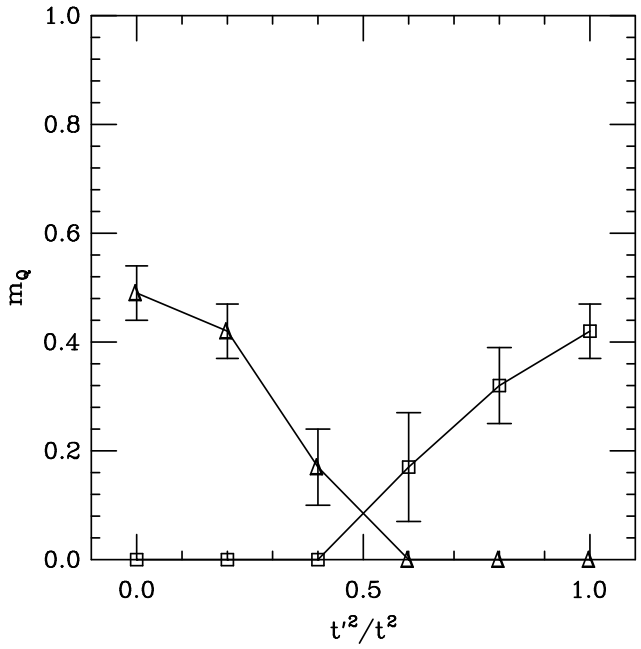

Figure 4. The staggered and layered magnetizations m_Q and m_X of the U–t–t' model on a square lattice for $U = 8t$. While the staggered magnetization m_Q vanishes for large t', the system will instead show layered Néel order m_X. On our scale, the classical Néel state takes the value of 1. Lines are purely guides to the eye.

In the following, we will discuss the ground-state energy and the staggered and layered magnetizations which were computed according to equation (9), for large and medium values of the correlation strength U as a function of t'^2/t^2. In the limit of large correlations and at half-filling, the U–t–t' model becomes the J_1–J_2 model with $J_1 \sim t^2/U$ and $J_2 \sim t'^2/U$. We therefore chose to express our data in terms of t'^2/t^2.

In figure 3 the ground-state energies of systems of linear sizes $L = 4$, 6, and 8 are plotted for strong correlations $U = 8t$. At $t' = 0$ we recover the bare Hubbard model with nearest-neighbour hopping, and the J_1–J_2 model will map onto the Heisenberg antiferromagnet. Our value for the energy at $t' = 0$ is in agreement with the data from previous QMC simulations made on the basis of the Hubbard model [5]. If the next-nearest-neighbour hopping is turned on, the system becomes frustrated as the magnetic disorder of the antiferromagnetically ordered system increases. Accordingly, the ground-state energy of the system will slightly increase. We observe that for $t'^2 \approx 0.5t^2$ the ground state reaches its maximum value, showing that for this value of t' the system has its maximum frustration. This can be understood in terms of the classical version of the J_1–J_2 model where the ground state changes from the Néel state to a layered Néel state at exactly $J_2 = 0.5J_1$.

If $t'^2 > 0.5t^2$, then the next-nearest-neighbour hopping dominates over the nearest-neighbour hopping, decreasing the frustration and the energy of the system again. The behaviour of the energy corresponds to that of analytical results [16] as well as numerical results from exact-diagonalization studies [12] of the J_1–J_2 model. It should be mentioned that there are finite-size effects in our simulations, but they are small.

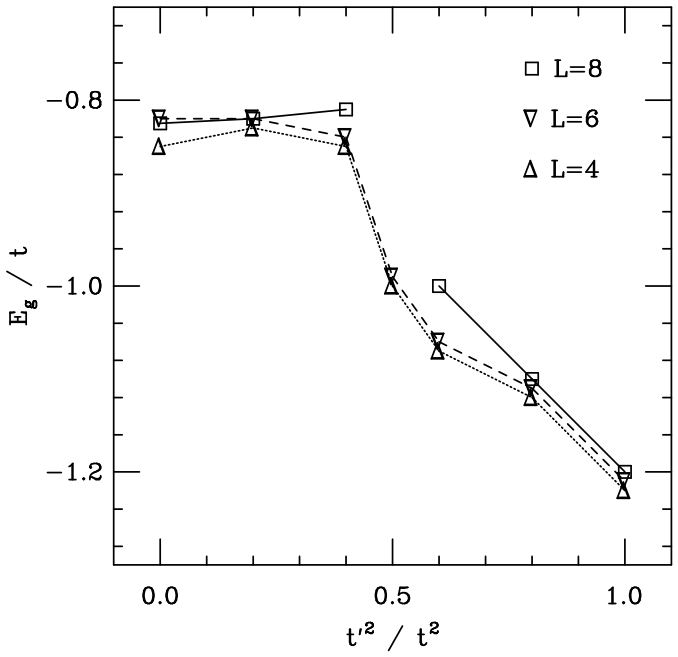

Figure 5. The ground-state energy per site of the U–t–t' model on a square lattice for $U = 4t$. The same error bars apply as in figure 3.

Let us now turn to the magnetic properties. In our simulation we compute the spin–spin correlation function

$$S(\boldsymbol{q}) = \frac{1}{N}\sum_{i,j} \mathrm{e}^{\mathrm{i}\boldsymbol{q}\cdot(\boldsymbol{R}_i - \boldsymbol{R}_j)} \langle (n_{i\uparrow} - n_{i\downarrow})(n_{j\uparrow} - n_{j\downarrow})\rangle. \tag{10}$$

In order to extrapolate to the thermodynamic limit, we plot $S(\boldsymbol{q})/N$ versus $1/N$ for linear system sizes $L = 4$, 6, and 8 [25, 5, 7]. It should follow a straight line according to

$$S(\boldsymbol{q}) = N m_q^2 + S_c(\boldsymbol{q}) \tag{11}$$

where S_c is the connected structure factor and m_q the magnetization:

$$m_q = \frac{1}{N}\sum_{i} \mathrm{e}^{-\mathrm{i}\boldsymbol{q}\cdot\boldsymbol{R}_i} \langle n_{i\uparrow} - n_{i\downarrow}\rangle. \tag{12}$$

From the extrapolated value for $N \to \infty$, we obtain the square of the magnetization m_q. We have followed this procedure for $\boldsymbol{q} = \boldsymbol{Q}$ and $\boldsymbol{q} = \boldsymbol{X}$ to obtain the staggered and layered magnetizations, respectively.

In figure 4 we depict the staggered and layered magnetizations m_Q and m_X for $U = 8t$ as a function of t'^2/t^2. At $t' = 0$, the system clearly demonstrates Néel order since the staggered magnetization takes on a finite value while the layered magnetization vanishes. If we increase the diagonal hopping amplitude t', the antiferromagnetic order of the system slowly decreases and a layered antiferromagnetic order develops, starting at around $t'^2 \approx 0.5t^2$. At $t'^2 \approx 0.5t^2$ the two types of magnetic order could coexist. Above $t'^2 \approx 0.6t^2$ the antiferromagnetic order is destroyed and the layered antiferromagnetic order

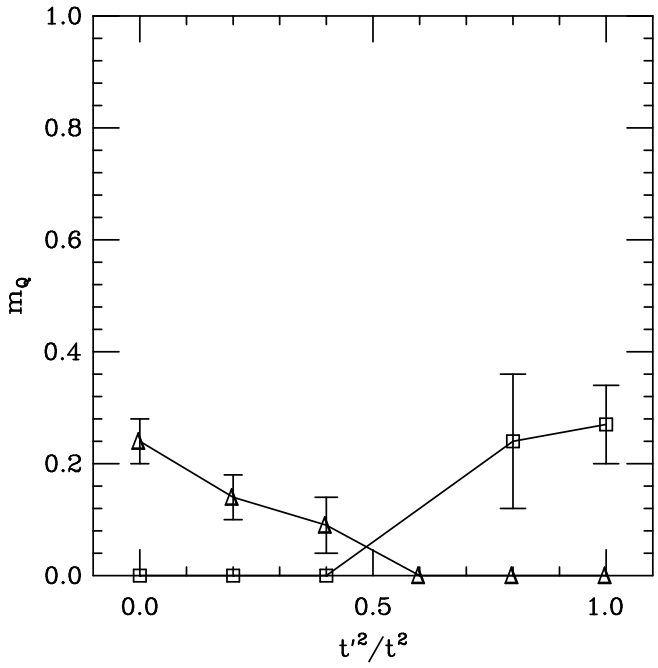

Figure 6. The staggered and layered magnetizations m_Q and m_X for $U = 4t$. See the description in the caption of figure 4.

dominates. The behaviour that we observe is in good agreement with a recent analysis [16] of the J_1–J_2 model. In the region where the transition between the two types of magnetic order occurs, the sign problem becomes serious, making it difficult to reach large enough β. Our data are not sufficiently accurate to allow us to specify the type of transition, i.e. whether it is a first- or second-order phase transition or a crossover between the two magnetic regimes [14]. Furthermore, the hypothesis of Dagotto and Moreo [12] of a spin-liquid phase around the critical point $\approx 0.5J_1$ in the J_1–J_2 model cannot be investigated.

The regions of intermediate correlation strength U are of much current interest [10, 11] since this parameter regime is believed to apply to the copper oxide planes. We therefore extended our calculations down to $U = 4t$. In figure 5 we have plotted the ground-state energy as a function of t'^2/t^2. In general, the behaviour is the same as for $U = 8t$: after a slight increase of E_g up to $t'^2 = 0.2t^2$, E_g decreases even more quickly than for $U = 8t$. Note that the maximum of the ground-state energy occurs in the range $t'^2 \approx (0.2 \ldots 0.4)t^2$, indicating that the critical region is shifted to smaller values of t'^2/t^2. We observe that for $L = 8$ the ground-state energy is considerably higher than for $L = 4$ and 6 at $t'^2 = 0.4t^2$ and $0.6t^2$. In this regime the system is highly frustrated and therefore the number of low-lying energy states increases. This number depends on the linear system size and makes it necessary, for large systems sizes, to use large projection parameters β, which are, however, not accessible due to the sign problem.

The different magnetization order parameters for $U = 4t$ are depicted in figure 6. The behaviour is, in general, similar to that for $U = 8t$, showing a transition between Néel and the layered Néel type of order at $t'^2 \approx 0.5t^2$. We observe that the magnitudes of the

staggered and the layered magnetizations are smaller than their counterparts for $U = 8t$, because the correlation strength is reduced.

5. Summary

To conclude, we have investigated the U–t–t' model using the projector quantum Monte Carlo method at strong and medium correlations. We introduced a SDW mean-field approximation with variational parameters m_Q *and* m_X. This was used to construct a trial state for the PQMC method in order to reduce the severity of the 'minus-sign' problem and to compute the staggered and layered magnetizations m_Q and m_X.

For the case of strong correlations, the system undergoes a transition from an antiferromagnetically ordered state to a layered antiferromagnetically ordered state as a function of t'^2/t^2. Extending the simulations to medium correlations, the same behaviour is observed, but showing a smaller magnitude of the magnetizations. Our results for the strongly correlated case agree well with analytical and numerical results for the J_1–J_2 model.

Acknowledgments

Support from the Deutsche Forschungsgemeinschaft is gratefully acknowledged. The authors thank K W Becker and H Köhler for helpful discussions and valuable comments.

References

[1] Bednorz G and Müller K A 1986 *Z. Phys.* B **64** 188
[2] Hubbard J 1963 *Proc. R. Soc.* A **276** 283
Hubbard J 1964 *Proc. R. Soc.* A **281** 401
[3] Hybertsen M S, Stechel E B, Foulkes W M C and Schlüter M 1992 *Phys. Rev.* B **45** 10 032
[4] Bénard P, Chen L and Tremblay A-M S 1993 *Phys. Rev.* B **47** 15 217
[5] Hirsch J E 1985 *Phys. Rev.* B **31** 4403
[6] Lin H Q and Hirsch J E 1987 *Phys. Rev.* B **35** 3359
[7] Hirsch J E and Tang S 1989 *Phys. Rev. Lett.* **62** 591
[8] White S R, Scalapino D J, Sugar R L, Loh E Y, Gubernatis J E and Scalettar R T 1989 *Phys. Rev.* B **40** 506
[9] Moreo A, Scalapino D J, Sugar R L, White S R and Bickers N E 1990 *Phys. Rev.* B **41** 2313
[10] Duffy D and Moreo A 1995 *Phys. Rev.* B **52** 15 607
[11] Duffy D and Moreo A 1996 *Phys. Rev.* B **55** R676
[12] Dagotto E and Moreo A 1989 *Phys. Rev.* B **39** 4744
[13] Dagotto E and Moreo A 1989 *Phys. Rev. Lett.* **63** 2148
[14] Schulz H J and Ziman T A L 1992 *Europhys. Lett.* **18** 355
[15] Richter J 1993 *Phys. Rev.* B **47** 5794
[16] Köhler H and Becker K W 1997 *Phys. Rev.* B **56** 8876
[17] Becker K W and Fulde P 1988 *Z. Phys.* B **72** 423
[18] For a recent review, see
von der Linden W 1992 *Phys. Rep.* **220** 53
[19] Fulde P 1995 *Electron Correlations in Molecules and Solids* (Berlin: Springer)
[20] Brenig W 1995 *Phys. Rep.* **251** 153
[21] Trotter H F 1959 *Prog. Am. Math. Soc.* **10** 545
[22] Suzuki M 1976 *Prog. Theor. Phys.* **56** 1454
[23] Hirsch J E 1983 *Phys. Rev.* B **28** 4059
[24] Metropolis N, Rosenbluth A W, Rosenbluth M N, Teller A and Teller E 1953 *J. Chem. Phys.* **21** 1087
[25] Oitmaa J and Betts D 1978 *Can. J. Phys.* **56** 879